

# The Contribution of CMR to Patients Undergoing the Surgical Ventricular Restoration (SVR) Procedure; One Center's Experience over Five Years

Robert W.W. Biederman\* and Mark Doyle

*Center for Cardiovascular Magnetic Resonance Imaging, Division of Cardiology, Department of Internal Medicine, Gerald McGinnis Cardiovascular Institute, Drexel University College of Medicine, 320 East North Avenue, Pittsburgh, PA 15212, USA*

**Abstract:** The use of Cardiovascular Magnetic Resonance (CMR) for the interrogation of the cardiovascular system is well established. As surgical techniques evolve seeking to address ischemic cardiomyopathic patients with increasing levels of cardiac functional perturbations, an imaging technique that is sufficiently comprehensive to complement these approaches is obligatory. The utility of CMR is shown for the evaluation of structure, function, morphology, viability, and intramyocardial strain by radio-frequency tissue tagging for patients with ischemic cardiomyopathy who are potential candidates for Surgical Ventricular Restoration (SVR). Using examples from the authors' experience over the last five years, representing perhaps the longest consecutive application of CMR to this complex patient group, the elements of a complete cardiac interrogation are demonstrated. Future applications for CMR aimed at the ischemic cardiomyopathic patient population are discussed, including applications to measuring diastolic function, stem cell research, and introduction of the concept of an energy model seeking to account for the mechanisms of the observed mechanical efficiency following SVR.

**Keywords:** Surgical ventricular restoration procedure, cardiovascular magnetic resonance imaging, ischemic cardiomyopathy, left ventricular dysfunction, dor procedure.

## INTRODUCTION

The Achilles' heel of cardiovascular magnetic resonance imaging (CMR) is its extreme sensitivity to motion. Unlike neurological and orthopedic applications, the heart is in constant motion, requiring extensive accommodation of motion from extrinsic (respiratory) and intrinsic (bulk cardiac motion) sources, all of which impact visualization of cardiac structures. Synchronization of the complex cardiac and respiratory motion in three dimensions is critical, requiring integrated gating algorithms, which have evolved over the preceding 15 years, and are still in evolution, overcoming the earlier limitations of CMR to acquire registered cardiovascular data. Currently, images are typically gated to the ECG-R wave and breathhold acquisitions are employed.

The maturity of the technological advances in CMR has permitted unparalleled access to be gained in the detection and assessment of ischemic heart disease [1-3]. Indeed, CMR has been the catalyst for surgical approaches for cardiac patients, who heretofore were considered inoperable.

Here we detail advances in CMR that are applicable to patients considered for the Surgical Ventricular Restoration (SVR) procedure proposed by Cooley [4] and Jatene [5] and, and modified into its present form by Vincent Dor [6], who developed the LV endoventricular circular patch-plasty approach. We detail the utility of CMR for patient selection,

surgical planning and post-surgical evaluation, incorporating examples from our lab, and the work of other investigators.

## LV STRUCTURE AND FUNCTION IN ISCHEMIC CARDIOMYOPATHY

The applicability of CMR for evaluation of the ischemic cardiomyopathic patient is outlined in Table 1. For over a decade, CMR has been widely regarded as the 'gold standard' for assessment of cardiac volumes and myocardial structures (Fig. 1) [7, 8]. Measurements of cardiac dimensions and volumes are highly reproducible using CMR, and when used to document changes in patient groups, allow an order of magnitude fewer patients to be followed to achieve similar statistical significance to less reproducible approaches [9]. Resultant usage and widespread adoption across the world has resulted in CMR becoming the test of choice for many clinicians and researchers [10]. Accurate quantification of LV volumes at end-diastolic and at end-systolic permit quantification of LV functional metrics such as stroke volume and ejection fraction, and these can be followed over time to sensitively document changes (Fig. 2). This aspect is particularly applicable for the quantification of left ventricular hypertrophy. Left ventricular mass can be calculated from CMR images by subtracting the epicardial shell from the endocardial shell to calculate volume, and convert this to mass by incorporating the specific gravity of myocardium (1.055). LV mass has been shown to be an important predictor of morbidity and mortality for patients with hypertension [11, 12], aortic stenosis [13], aortic regurgitation, mitral regurgitation [14], and hypertrophic cardiomyopathy [15]. For the patient with ischemic cardiomyopathy, such considerations have further value

\*Address correspondence to this author at the Center for Cardiovascular Magnetic Resonance Imaging, Division of Cardiology, Department of Internal Medicine, Gerald McGinnis Cardiovascular Institute, Drexel University College of Medicine, 320 East North Avenue, Pittsburgh, PA 15212, USA; Tel: 412-359-8009; Fax: 412-359-6358; E-mail: rbiederm@wpahs.org

when resolution of the often thin myocardial wall retards correct measurements. The ability to detect wall motion defects when myocardial wall thickness is eccentrically remodeled has historically hampered identification of resting and/or augmented myocardial reserve.

**Table 1. Characteristics of CMR Applicable to the Ischemic Cardiomyopathic Ventricle**

CMR Imaging Characteristics	
"Gold Standard" For Cardiac Function	
	LV/RV function
	LV mass
	Viability (delayed hyperenhancement)
Reproducible	
	No limitations of 'window' or body 'habitus'
	Applicable to the asymmetric LV
	Inherent 3D resolution
No ionizing Radiation	
	No x-rays
	No iodinated contrast required
	No radionuclide agent

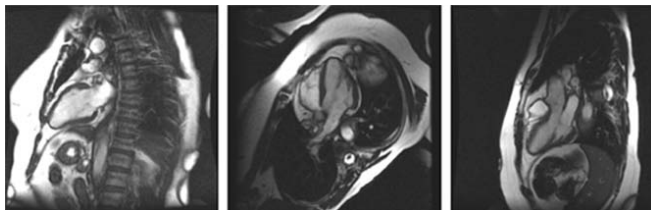


**Fig. (1).** CMR images depicting 2, 4 and 5 chamber images using a SSFP (Steady-State Free Precession) technique with a 12-14 second breath-hold. No IV, contrast, radiation, or catheters are required to produce these CMR images.

In our era of ejection fraction serving as a threshold metric, i.e.; EF >40% is treated less aggressively than that of a patient with an EF <40%, it is particularly important to possess fluency with a modality that has a variability in the sub-clinical range. Specifically, most current modalities report ejection fractions with variabilities in excess of 10-15%, regardless whether measured or estimated [16-18]. This may improve with the use of contrast imaging [19]. In numerous studies, EF variability by CMR has been shown to be below 5%, indeed often below 2% [20, 21]. Our center served as the core CMR Lab in the recently published 4E Trial [22], testing the effects of individual or combination eplerenone and enalapril, both selective renin-angiotensin-aldosterone system activity inhibitors regarding LVH regression and blood pressure control. We reported standard

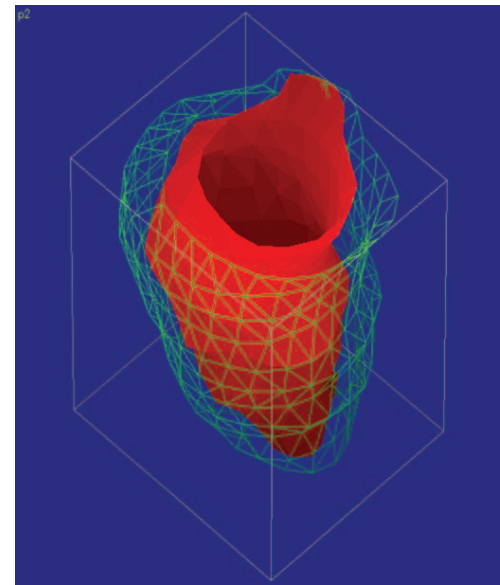


**Fig. (2).** Three-dimensional formulation of a normal LV depicting the endocardium (inner solid contour) and the epicardial shell (outer triangulated skeleton). Evaluation of 3D geometry in terms of structure, function and geometry are common-place using standard analysis packages available on most CMR systems for patients referred for complex surgical reconstruction. This image is derived from our Medis software (The Leiden, The Netherlands package on our GE EXCITE 1.5 T system, Milwaukee, WI).

errors for LVEF of 1.5% and LV mass of 5.0g. In some laboratories, CMR has been demonstrated to have no more than a 4g change over the entire cardiac cycle (20 phases) demonstrating the reproducibility and preservation of mass within tolerable limits to an exceptional degree (personal communication with Alistair A. Young, Ph. D, Auckland University, New Zealand).

CMR is not only an excellent technique to depict myocardial necrosis and scar tissue, as we shall see in patients with ischemic heart disease, but there is evidence to suggest a better identification of LV apical thrombi in patients with ischemic cardiomyopathy than with presently used clinical imaging modalities, such as echocardiography [23]. The spatial resolution afforded when combined with the T1 effect (bright) sandwiched between the dark myocardial/pericardial border and the dark thrombus is pathognomonic for thrombus far exceeding the limited tissue characterization afforded by techniques based on ultrasound (Fig. 3).

With rapid imaging becoming an integral request for the evaluation of ischemic cardiomyopathy, requests to perform such exams occur more frequent, often representing a sicker, more complex patient clientele. While standard CMR imaging is improving acquisition speed, a faster technique we have developed named BRISK (block regional interpolation scheme for k-space) [24] utilizes a sparse sampling technique with high interpolation factors (up to five currently) to generate unsampled data through interpolation strategies from unnecessary data in the k-space domain. We have shown that BRISK can reduce the scan time by 70% compared with a conventional CMR scans. Further, utilizing turbo-BRISK scans, with segmentation factors up to 5, the

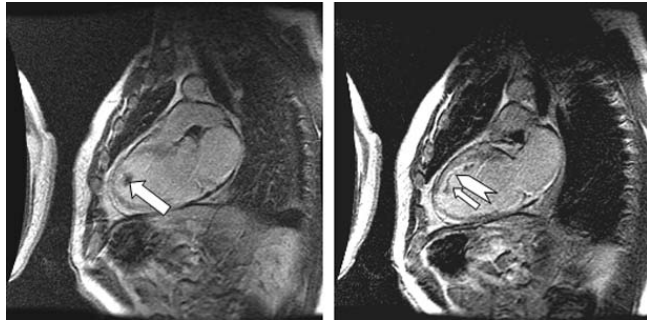


**Fig. (3).** **A**) In a patient with ischemic cardiomyopathy, there is a large apical, mobile mass adjacent to anterior apical thinned myocardium (arrow). **B**) In the same patient using delayed hyperenhancement, slightly lateral, there is clot (dark) seen adherent to endocardial scar (bright) (chevron). Excellent dichotomization between viable and non-viable myocardium is possible, and has been shown recently, extremely high sensitivity and specificity for determining LV thrombus is possible markedly exceeding transthoracic and transesophageal echocardiography.

scan time can be reduced by up to 94%. Recently, this concept was validated *in vivo* with 10 patients [25].

### LV Geometry by CMR

It has been well established that CMR is the gold standard for the evaluation of LV (and RV) systolic function. The accuracy, reproducibility and ease of detection by CMR, when the diagnosis of a dilated ischemic cardiomyopathy is relevant, are self-explanatory. What is less clear is how those in whom the diagnosis may not be apparent may be erroneously classified if less rigorous imaging techniques are applied. Testing this specifically, we asked the question, "Does end-diastolic dimension (EDD) misguide the estimation of end-diastolic volume (EDV) in Patients with Ischemic Cardiomyopathy?" For normal (NL) left ventricles it is assumed that 1D=3D believing normal hearts possess a symmetrical ellipse of rotation; a prolate ellipse of rotation. Yet, patients with a dilated ischemic cardiomyopathy (CMX) seldom have symmetrical LV's. Despite this, unfortunately, EDD is used as a threshold value to distinguish NLS from CMX in clinical practice. Is this correct?

Seeking an answer, we compared EDD by echocardiography (Echo) and CMR against EDV by CMR. A total of 28 subjects were enrolled, 14 consecutive CMX pts ( $60 \pm 6$  yr) referred for the Dor procedure and 14 normals (NL) ( $50 \pm 16$ yr). CMR and Echo were performed within  $1.6 \pm 4.3$ mo of each other. Echo was measured using ASE conventions and CMR EDV was measured using Simpson's Rule. EDD for NLs and CMX was:

$41 \pm 5$  and  $61 \pm 9$  mm by Echo and  $44 \pm 3$  and  $66 \pm 7$  mm by CMR The EDV for NLs and CMX was  $101 \pm 20$  and  $265 \pm 78$  ml by CMR. The correlation for the pooled population for EchoEDD and CMREDD against EDV was  $r = 0.84$  ( $p < 0.001$ ). The individual regression analysis for EchoEDD vs. EDV showed a standard error of  $\pm 55$ ml while for CMR EDD vs. EDV the standard error was  $\pm 44$ ml. This demonstrates that for any individual there is poor prediction of EDV, i.e. by Echo, 2 CMX and 3 NLs (18%) and by CMR, 1 CMX and 3 NLs (14%) were misclassified. Thus, the 1D

measurement of EDD, either by Echo or by CMR, while highly correlated, is a poor predictor of volume, not only for patients with CMX, but also in NLs. Reliance on 1D measurements can result in erroneous 3D volume estimates (Fig. 4). This strongly suggests that EDV should be the mainstay for the evaluation of patients with CMX. It is based on this analysis, when combined with other data supporting the complete interrogation afforded by CMR, no patient will undergo SVR at our hospital prior to such an evaluation. Though we were among the first to adopt such a practice in the world [26] others have quickly followed around the world, such that if one wishes to know the answer regarding specific SVR related questions, CMR is the definitive tool.

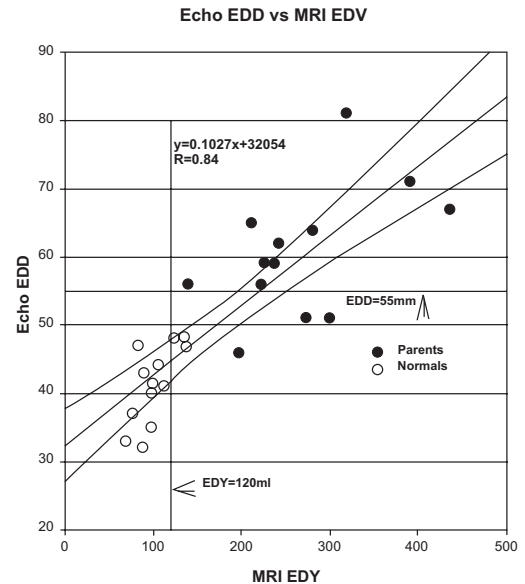


**Fig. (4).** Representing the poor diagnostic accuracy to depict 3D volumetrics via any 2D method, this graph demonstrates the marked inability for an LV end-diastolic dimension of 55mm (the 1D upper limit of normal) to predict a normal volume. This concept works in reverse; in an asymmetric ventricle, a volume  $> 120$ ml often does not conform to an LVEDD of 55mm. The cardinal notion is that in the markedly asymmetric ventricle, over reliance on 1D measurement often incorrectly predicts that the LV is smaller than necessary for consideration for LV reconstruction. In our facility, all patients undergoing consideration for such advanced surgery undergo CMR for this reason, amongst many. (Statistical courtesy to Diane A. Vido, MS, Allegheny General Hospital, Pittsburgh, PA).

### LV Intramyocardial Strain Evaluations

Intramyocardial function is dependent upon fiber orientation and chamber geometry in addition to the more classical chamber function estimates. The sum total of these interactions yields the ejection performance we can measure at the bedside. One of the most unique capabilities of CMR, although not yet a bedside tool, is the interrogation of intramyocardial function by LV strain measured *via* radio-frequency (RF) tissue tagging. The contribution of a high resolution imaging technique to the assessment of regional wall function afforded by CMR RF tagging may be unparalleled (Fig. 5). Traditionally, tantalum markers or implanted radio-opaque markers are required to identify material points

within the heart. Typically this is performed in a limited capacity in animals. Implantation of sonomicrometry piezoelectric ultrasound crystals are also employed again in the experimental animal model. Using identifiable cardiac markers such as epicardial coronary tracking has been utilized but in limited fashion. CMR tissue tagging permits the placement of thousands of material points across the LV in a non-invasive manner permitting quantitation of complex myocardial deformation such a radial, circumferential and longitudinal (meridional) strain [27]. These can be further refined into principle major and minor strain relating myocardial deformations, not only in the Cartesian coordinate system (x, y, and z) but deconvoluting principle vectors of deformation into maximum and minimum strains. Further consideration can be made for defining the strain related to the finite starting point of the relaxed state, end-diastole, to that at end-systole; related only to the undeformed strain termed Lagrangian strain. Strains can be decomposed into principle strains or orthogonal eigenvectors. The deformation of a hypothetical circle into an ellipse gives us the major and minor ax that corresponds to the strain directions and are the eigenvectors of the transformation with their lengths being the eigenvalues. In Eulerian (natural ) strain, the reference value is not constant over time but changes during the deformation process. In the case where the rate of deformation is constant as a function of time, the Lagrangian strain  $EL(t)$  and the Eulerian strain  $EN(t)$  have a non-linear relationship. Redefining strain for the heart, the latter allows for more heterogeneous determination of intramyocardial function but at the expense of considerable more time point estimations whereas the former permits a homogeneous assumption between material points simplifying analysis. More complete evaluations using either manner can be defined by using finite-element modeling in both 2D and 3D quantifications [28] (Figs. 6 and 7). Additionally, CMR radio-frequency 1, 2 or 3D tissue tagging allows for the deconvolution of bulk cardiac motion (rotational and translational) which may be greater in magnitude than the local myocardial deformation. With its' very recent arrival into the imaging world, echo-

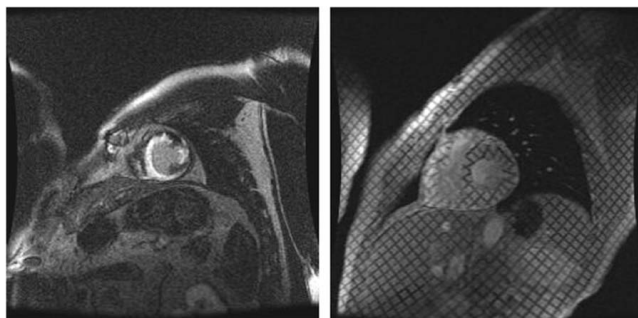


**Fig. (5).** A middle aged male presented with a large anterior and anteriorseptal MI for which he underwent urgent PTCA. Shown is the delayed hyperenhancement (0.2mMole/kg Gadolinium injected 2 days after infarction (A) The white signal is the bright T1 signal due to extensive, nearly transmural scar. Note the striking ability for CMR to depict with high spatial resolution the underlying transmural of the infarct, easily distinguishing b/w normal (dark) and scar (bright) myocardium In (B) is the corresponding radio-frequency tissue tagging images depicting information about intramyocardial deformation.

cardiography strain is in its' infancy, relegated to only 1D approaches, without regard for bulk cardiac motion, translational, shear, or torsion consideration.

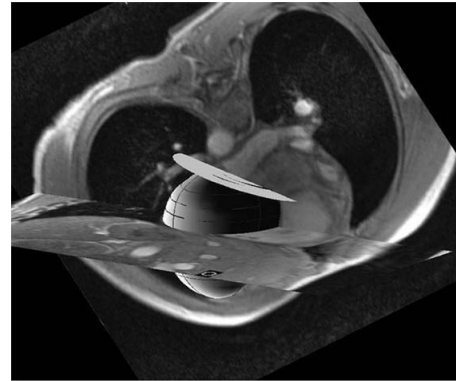


**Fig. (6).** Finite element modeling depicted in 3D with interweaving orthogonal slices integrating both LV structure, form and function. (Courtesy of Alistair A. Young, PhD, Auckland University, Auckland, New Zealand).



**Fig. (7).** A 3D finite-element analysis depicting the evolution of LV shape, volume and wall thickness from pre-SVR, 1 month and one year. From this circumferential, radial, and meridional strains can be derived with their underlying volumetrics. (Courtesy of Alistair A. Young, PhD, Auckland University, Auckland, New Zealand).

Analogous to the development of CMR has been the sophistication in post-processing permitting advancements from earlier manual quantifications, which often required in excess of 40 hours per patient to now less than 1hour per patient. The resultant measurements provide a measurement of regional myocardial wall function and can be mathematically expressed in terms of a tensor while visually displayed as a vector or a color schema [29, 30].

Seeking to determine the relationship between altered LV volumetric indices and changes in regional intramyocardial function using such intramyocardial strain in patients undergoing surgical ventricular reconstruction therapy, we studied 15 patients ( $59 \pm 5$  years-12M,3F) referred for the SVR procedure at  $1 \pm 1d$  prior (Pre),  $2 \pm 1mo$  (Post) and  $1 \text{ year} \pm 5mo$  (Late). Two patients had a mitral valve replacement and all but one had CABG. End-diastolic volume, end-systolic volume, stroke volume, and ejection fraction (EDV, ESV, SV, and EF) were measured. A subset of six patients underwent 3D CMR radio-frequency tissue tagging (Fig. 8). Circumferential, radial, meridional, and circumferential-longitudinal (CL-shear) strains were measured using finite-element analysis. Principal minor and major strain was calculated from the strain tensor oriented in the circumferential direction. Specific investigation was directed towards the role of

the reconstructed ventricular geometry. The LV was then divided into three regions: the Repair site, Adjacent and Remote myocardium.

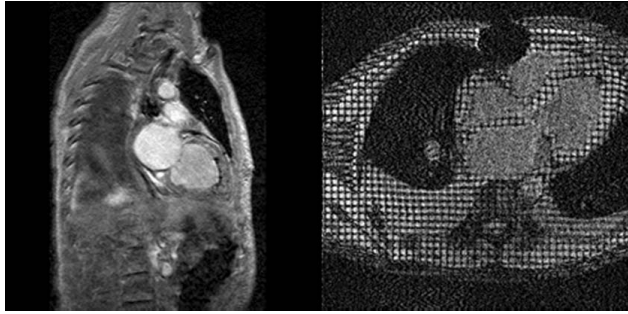


**Fig. (8).** Following SVR, the evidence of the patch is visible as a small black line at the ventricular apex. The orthogonal image with radio-frequency tissue tagging is shown of the same patient, again the patch is just visible at the apex but note the paradoxically thickened apex due to the apical wrap but not exclusion of the formerly akinetic and thinned, scarred LV. The paramagnetic artifact of the sternal wires is present anteriorly as a black circular defect. Note the bilateral pleural effusion in this early post-operative period. These resolved over the next 3 weeks.

After the Dor procedure, EDV and ESV decreased while SV and EF increased (see Table 2 and Fig. 8). Circumferential strain increased in the Remote but not the Adjacent or Repair regions by 19%: ( $7.3 \pm 2.4$  to  $8.7 \pm 2.3$ ,  $p < 0.05$  with no significant increase Late ( $8.9 \pm 2.1$ ). Meridional strain at the Repair site showed lengthening Post and a trend towards shortening Late with no significant changes in Adjacent or Remote regions. An increasing gradient in radial strain between Repair and Remote through Pre, Post and Late was present ( $p < 0.05$ ). CL-shear was unchanged. Maximum principle strain increased at POST and remained so at follow-up ( $10 \pm 4$  to  $15 \pm 2$  to  $14 \pm 5$ , ( $p < 0.005$  for all). There was no significant difference in minimum principle strain. Phi, the angle between the circumferential direction and the minimum principle strain, changed PRE to LATE from  $-21 \pm 16$  to  $-10 \pm 22$ , ( $p < 0.005$ ) becoming globally more circumferential. However, regionally, Phi become oriented more longitudinally and directly correlated with distance from the surgical patch (Repair). This indicated that, following SVR in patients with end-stage ischemic cardiomyopathy, reverse remodeling occurs which is coupled with improvements in intramyocardial mechanics predominantly in the remote myocardium at one year.

**LV Myocardial Torsion by CMR**

One of the most unique aspects of CMR evaluation of the LV is the ability to evaluate fiber interaction *via* analysis of

LV torsion. In diastole, before valve opening (during isovolumic relaxation) pressure decay is related to “untwisting”. Untwisting may be, in part, responsible for LA pressure decay and for Tau (T). The early reduction in LV torsion has been suggested as a marker of future LV dysfunction and by CMR directly related to Tau.

Believing that restoration of fiber orientation, as a chief element desirous of favorable outcome following the SVR procedure is important, we undertook a CMR evaluation of such. Resumption of perturbed fiber orientation theoretically might be measured and represented as the sum interaction and integration of LV torsion. Torsion is usually derived in one of two manners, as a measure of circumferential-longitudinal shear (CL shear) derived from the arctangent of the difference of the slope between the basal and any subsequent plane when connected to the centroid was the torsional angle ( $^{\circ}$ ). This technique is corrected for rigid body rotation and translation. A second method is one that we exploited and describe below. The cardinal point is that either technique conveniently described that which excludes description by *any* conventional clinical technique to date, including angiography, echocardiography or nuclear modalities. Along with a colleague of ours, Dr Agustino Meduri from Italy, we looked at 14 patients with end stage ischemic cardiomyopathy undergoing SVR *via* radio-frequency tagged CMR. The development of torsion(Tdev(degrees/mm)) was calculated as was the absolute change in torsion Torsion(degrees) from base to apex by measuring the angular rotation (relative to the centroid and referred to the base) for four midwall segments equally positioned around each short axis slice (CL shear ) to analyze 3D torsion. We showed that typically, torsion increased from base to apex (12 of 13 patients), with the apex experiencing the most torsion. After surgery the average LV length decreased ( $83_{16}$  vs.  $65_{10}$ mm  $p < 0.01$ ) as did CL-shear ( $10_{60}$  vs.  $6_{30}$   $p < 0.05$ ) while the Tdev was unchanged ( $0.16_{0.1}$  vs.  $0.15_{0.06}$ ), (Fig. 9). Unfortunately, by this analysis, despite buttressed by an intact rationale, no evidence for restoration or improvement of torsion could be elucidated by scrutinizing torsion. Reconsideration for this analysis takes center stage as it is now clear that a portion of these patients had the aforementioned “snub-nosed” LV. A later subset analysis of the patients with the most favorable LV geometry revealed redemption of the initial hypothesis.

The role of changing LV geometry has not been extensively studied when directly considering the post SVR patient. In part, the elemental precept underpinning the SVR procedure incorporates realignment of circumferential and meridional fiber surgically coerced from spherical to the normal prolate ellipsoid geometry operational in the pre-morbid state. We assessed a CMR-derived geometric index in patients who underwent SVR [23, 31]. Fourteen subjects including six with ischemic CMX (end-diastolic dimension

**Table 2. Changes In LV Volumetrics Following SVR In 15 pts at 12±5 Months by CMR**

	LVEDV (ml)	LVESV (ml)	SV (ml)	EF (%)
PRE	246±45	218±36	78±10	24±4
POST (12±5mo)	210±26*	143±18*	90±12*	32±6*

A \* indicates a  $p < 0.05$  (pre vs. post).

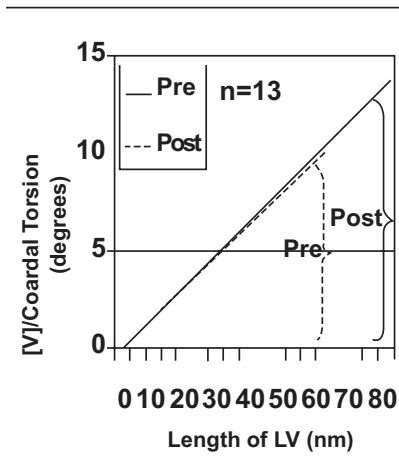


**Fig. (9).** CMR demonstrating circumferential-shear (Torsion) depicting a reduction in maximum torsion (experienced at the apex) but, when integrated at torsion per mm (of long axis), there was no change between patients pre-SVR and post-SVR, eliminating that consideration as a major explanation why patients had a return to function following the SVR procedure.

66±6mm, end-diastolic volume 282±40ml, ejection fraction 20%, NYHA mean 3.3) were compared to 8 normals all who underwent a similar CMR evaluation. A global prolate ellipse was fit to each LV in the 2-chamber and 4-chamber view using the major and minor axes at the base. Secondly, an apical prolate ellipse was fit to a section positioned at 2/3 of the major axis to more appropriately define the newly reconstructed apical geometry. Finally, the ratio of the apical/global minor axis ellipses in each projection characterizing the agreement (or amount of heterogeneity) between the two prolate ellipses was examined. Consequently, as the ratio approaches unity, the apical ellipse approximates the global ellipse, implying that the apical shape precisely tracks the global geometry. (Fig. 10) shows the mean±SD apical/global geometric indices for the patients pre and post SVR compared to a normal population. Normal patients have a high degree of agreement between the idealized global ellipse and the apical ellipse regardless where one measures demonstrating preservation of intact

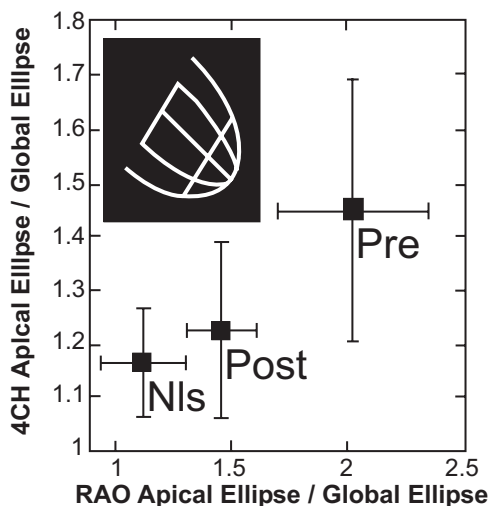


**Fig. (10).** SCMR Prolate ellipse.

basal to apical symmetry. Ischemic patients, on the other hand, while having an apparent prolate ellipse when measured at the base deviate far from normal the more apical one interrogates. Notably, we demonstrated that, as expected normals and ischemic CMX patients were significantly different when such a geometric analysis was applied by CMR. However, following CMR, the measured apical/global heterogeneity geometry index moved leftward and down, approaching that of normals and revealing a very strong trend towards LV geometric normalization. The CMR evaluation indicated that, in addition to simple volume reduction, geometric remodeling, surgically induced, is a significant component to the SVR [32, 33].

Such an observation proved key in the recognition that, despite a normalization of LV volume by the SVR, the attribute felt critically important by many, the final LV geometry, was still not ideal in some. Indeed, careful examination by CMR and other imaging techniques easily unveiled that an apical truncation process was often in effect. Simple recreation of the Fontan suture and surgical exclusion of the apex perpendicular to the long axis of the LV might result in a ‘snub nose’ LV defeating significant gains appropriated from a reduction in Laplacian stress [34].

#### Viability Considerations in the Ischemic Patient

The identification of patients with resting left ventricular dysfunction secondary to CAD who would benefit from revascularization versus surgical exclusion of that myocardium is paramount in clinical practice and for application of the SVR procedure. Generally, most investigators feel that a viability determination is a key component to such surgical decision making. If one can absolutely assure that viable myocardium is present, decisions regarding myocardial exclusion, interestingly, become more complex. If lack of viability is present, surgical exclusion with the SVR is an easy and rationale approach. However, currently, the clinical equipoise over whether volume or viability is superior when considering the SVR patient is a key question, actively being tested in the NHLBI funded STICH Trial. Data to suggest that volumetric considerations might supplant those of traditional viability gain credence form the observation by a number of investigators who show that end-systolic volume index >60ml/m<sup>2</sup> is a better index than ejection performance (EF) and/or the presence of viability in patients undergoing CABG only. Others have shown that, despite CABG, LV volume typically increases with a commensurate increase in the persistence of heart failure and an earlier than predicted mortality. Another less obvious considerations stems from our general imprecise measure of viability by current techniques. In that CMR has a spatial resolution at least 10-fold greater than current radionuclide agents thallium or sestamibi, clinical nuclear testing for viability is quite insensitive to the detection of sub-endocardial defects. Specifically, nuclear imaging in-plane spatial resolution is on the order of 12-13mm while CMR using gadolinium DPTA as its detector has in-plane resolution of 1-2mm. It follows that nuclear defects >one-half of that will be in the vicinity of the lower-most detectable by nuclear strategies. Thus, subendocardial defects or those approaching the midwall will be easily detectable by CMR. This calls into question the finding of a ‘normal’ nuclear examination by a nuclear

study. Especially for the precise delineation critically important for that patient potential for SVR, such correct determination is mandatory.

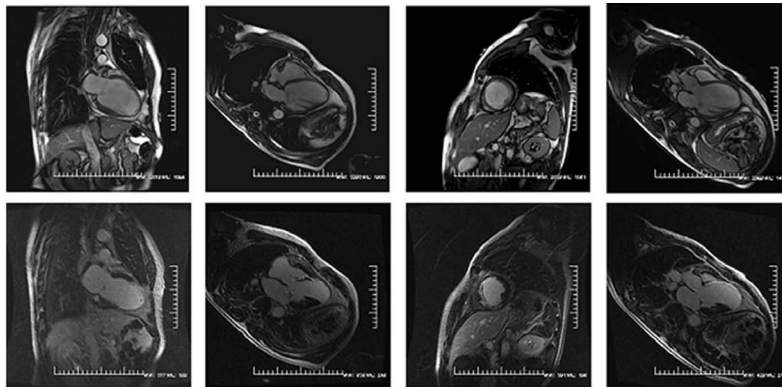
Further debate over whether resting myocardial blood flow is abnormal in "hibernating" myocardium or whether "hibernation" represents repetitive "stunning" is the topic of much current discussion in the scientific community [35]. What has become clear is that the myocardium in ischemic cardiomyopathy is made up of a combination of scarred, hibernating, and stunned myocardium. Within a given region of scar, there may exist patches or islands of viable myocardium. Once this is understood, it becomes clear why cardiac CMR is an ideal choice for the noninvasive assessment of myocardial viability (Fig. 11). We believe CMR is now the "gold standard" and the time for its widespread use in the assessment of myocardial viability is at hand. A comprehensive review of the seminal investigative studies which support this conclusion is beyond the scope of this review. Instead, we will focus on the recent literature illustrating the complementary role the different CMR modalities have on our ability to identify viable myocardium.

The concept that CMR can differentiate transmural infarction from subendocardial infarction because of its high spatial resolution was well-demonstrated in a recent study by Wagner *et al.* [36]. These investigators compared nuclear SPECT to contrast CMR in a canine infarct-reperfusion model as well as in a group of 91 patients with known or suspected CAD. Although both techniques detected transmural infarct with equal accuracy in the canine portion of the study, contrast CMR detected significantly more subendocardial infarcts compared to SPECT (92% vs. 28%)

when pathology was the 'gold standard'. In the human portion of the study, 47% of individuals with a clear subendocardial infarction by contrast CMR had no evidence of infarction by SPECT. Thus, contrast CMR systematically detects subendocardial infarcts that are overlooked by SPECT.

An important recent study by Klein and co-workers compared contrast CMR to PET, the historical "gold standard" for detection of viability in 34 patients with ischemic LV [37]. Hyperenhancement correlated closely with location and extent of infarct scar as assessed by PET with  $^{13}\text{N}$ -ammonia for perfusion and fluorodeoxyglucose (FDG) as a metabolic tracer. Here hibernating myocardium was identified correctly as viable by CMR in most cases. Once again, however, the distinction between CMR and PET came down to the superior spatial resolution of CMR, allowing more subtle delineation of scar than PET. Eleven percent of PET viable segments demonstrated subendocardial scar on contrast-enhanced CMR. Hyperactive metabolic subepicardial segments may mask subendocardial scar on PET imaging preferentially uptaking tracer, spuriously masquerading as 'viable' myocardium.

The relationship between these techniques and the prediction of functional recovery after revascularization is an area of active investigation. In a study by Kim *et al.* [38], the transmural extent of hyperenhancement on delayed contrast-enhanced CMR correlated inversely with functional recovery in 50 patients after revascularization, most of who had chronic ischemic disease. Segments without hyperenhancement had an approximately 80% chance of functional recovery, whereas segments with >50% transmural hyperenhancement had little likelihood of recovery following revas-



Patient Data: LVEDD: 63.3mm, LVESD: 51mm, LVEF=24.9%  
 LVEDV 245ml, LVESV 183ml, LVSV 62ml, LV Mass 135g  
 LVEDVI 137ml/m<sup>2</sup>, LVESVI 103 ml/m<sup>2</sup>, LVSVI 35 ml/m<sup>2</sup>, LVMI 75g/m<sup>2</sup>

**Fig. (11).** A 58 YO WM is referred for consideration of the SVR procedure and undergoes a CMR for volumetrics, function and viability. Shown (left to right) is 2, 3, 4 chamber and short axis on top row (SSFP) with viability (delayed hyper enhancement) on bottom row. Note the markedly dilated LV with eccentric remodeling due to thinning of anterior, anteroapical and anteroapical walls secondary to a large myocardial infarction. Evidence of the extent of the myocardial infarction is shown in the bottom rows where the infarct (white) can be easily discerned from the viable (dark) myocardium depicting a large amount of unsalvageable myocardium ((28% scar). The remaining non-infarcted walls were remodeled but still thick enough and of sufficient amount (>70%) of the myocardium to support an apical reconstruction approach that the SVR offered. The EF was predicted to increase from 27% pre-SVR to 41% post-SVR given then excluded anteroapical reconstruction. 4 weeks after the procedure the patients EF was 37% matched with a decrease in NYHA from NYHA III to NYHA I.

Patient Data: LVEDD: 63.3mm, LVESD: 51mm, LVEF=24.9%.

LVEDV 245ml, LVESV 183ml, LVSV 62ml, LV Mass 135g.

LVEDVI 137ml/m<sup>2</sup>, LVESVI 103 ml/m<sup>2</sup>, LVSVI 35 ml/m<sup>2</sup>, LVMI 75g/m<sup>2</sup>.

cularization. The predictive value of subendocardial infarction (1-50% transmural hyperenhancement) was lower and the dobutamine response in these segments might aid in the ability to assess the likelihood of functional recovery.

Recently we showed that viability by CMR contained predictive value of early delayed hyperenhancement following revascularization. As stated above, after a myocardial infarction (MI), gadolinium contrast magnetic resonance imaging (CMR) can reveal myocardial regions of delayed hyperenhancement (DHE). It is well known that the presence of DHE is associated with compromised myocardium but its interpretation remains controversial [39]. In particular the presence of DHE has never been demonstrated to be predictive of long term EF post intervention. Patients considered for SVR fall into this category, namely, if it is clear that a patient will not benefit in the peri-infarct period or, more appropriately within the next 1-2 months despite interventional techniques designed to accomplish such, a greater early pre-SVR planning period may be possible. Those who would be deemed SVR candidates potentially could be monitored in an expectant manner.

With this as a backdrop, we hypothesized that DHE regions consist of a combination of viable and non-viable myocardium and that congruence of myocardial wall function and the DHE distribution early after revascularization would be predictive of late-term myocardial function denoted by EF and intramyocardial function [40]. Ten patients (2 female) aged 38-69, post MI who received complete revascularization therapy by PTCA were studied. CMR was performed Early ( $2.6 \pm 1.2$  days post MI) and Late ( $7.4 \pm 1$  week post infarct). Images were obtained in the short-axis orientation to assess function and DHE extent. The endocardial and epicardial borders were planimeted and data extracted at 100 points around the circumference of each slice, analogous to the center-line method, to calculate end diastolic to end systolic wall thickening and record the DHE signal. For each slice we performed a correlation analysis to assess congruence of the DHE pattern and wall thickening at the Early time point. The EF was calculated using Simpson's rule.

The average correlation values of the DHE signal with wall thickening ranged from -0.51 to +0.33 (mean -0.15) with a negative correlation indicating low myocardial function in regions of DHE and a positive correlation indicated relatively high function in regions of DHE. At the Late time point, EF ranged from 38-68% (mean 55.2%). Linear regression analysis showed that the correlation of DHE and wall thickening, Early, was inversely related to EF at the Late time point, ( $r=0.8$ ,  $p<0.01$ ). Thus, Early post infarct, patients with a negative correlation of DHE with wall thickening were likely to beneficially remodel, while patients exhibiting a positive correlation were very likely to adversely remodel. The congruence of the DHE pattern and wall thickening Early post MI was not a binary response and can be used to predict ventricular EF at the Late time point leading to an increased precision in defining early in the time course those patients who may not benefit from traditional intervention, undergo late remodeling and potential candidates for SVR consideration.

The impact of such a refined tool by CMR has been recently demonstrated in CABG patients. In a clinical trial [41], 52 patients underwent multivessel CABG *via* either the off-pump or on-pump surgical technique. The patients were studied preoperative, early (day 6) and late (6 months) postoperative with CMR for global and regional functional assessment and delayed-enhancement CMR by gadolinium DHE for the assessment of irreversible myocardium. Preoperatively, 611 segments (21%) had abnormal regional function, whereas 421 segments (14%) showed evidence of hyperenhancement. At 6 months after revascularization, 57% (343 of 611) of dysfunctional segments improved contraction by at least 1 grade. When all preoperative dysfunctional segments were analyzed, there was a strong correlation between the transmural extent of hyperenhancement and the recovery in regional function at 6 months ( $P<0.001$ ). Of a total of 96 previously dysfunctional but nonenhancing or minimally hyperenhancing myocardial segments that did not improve regional function at 6 months, 35 (36%) demonstrated new perioperative hyperenhancement in the early postoperative MRI scan. This study demonstrated that DHE by CMR is a powerful predictor of myocardial viability pre-surgery and is predictive of late myocardial dysfunction incurred presumably in the peri-operative period. Taken together, this suggests an important role for this technique in clinical viability assessment prior to CABG surgery. Again, in our hospital, we as many across the world do, offer such a clinical evaluation prior to CABG and/or CABG/SVR.

A final point regarding the detection of ischemic heart disease and confidently distinguishing a patient from a non-ischemic patient was recently underscored by the ATLAS Trial [42] which sought to relate pre-morbid clinical diagnosis to post-mortem diagnosis. Ideally, these should match. Reading this trial carefully yields the incidence of significant CAD ( $>50\%$ ) by autopsy in non-ischemic cardiomyopathy patients was 13%. Similarly, the incidence of insignificant CAD ( $<50\%$ ) in ischemic cardiomyopathy patients by autopsy was 12%. Taken together, upwards of 25% of patients defined by classical x-ray coronary angiogram and/or nuclear examinations may be erroneously labeled portending markedly ineffective therapeutic strategies being implemented throughout the world.

### **Coronary Artery Imaging**

The identification of ischemic cardiomyopathy entails, by definition, the ability to detect CAD within the coronary lumen. While the latter has considerable limitations towards truly defining that property which governs the "high risk plaque", the luminal disease maintains prominence squarely in the center of the surgeon and cardiologist's mind as the most important information to glean. The morbidity and mortality surrounding the use of traditional x-ray angiography has been well described, yet unchanged over the last 2 decades, despite marked improvements in our technique, catheters and peri-catheterization strategies [43]. Thus, the ability for CMR to provide insight into detection of CAD has tremendous appeal and currently serves as our "holy grail" (Figs. 12 and 13). In a multicenter, international trial evaluating 7 centers in 109 patients with standard sequences on a one vendor study (Philips), the sensitivity, specificity, and accuracy for patients with disease of the left main coronary

artery or three-vessel disease were 100 percent (95 percent confidence interval, 97 to 100 percent), 85 percent (95 percent confidence interval, 78 to 92 percent), and 87 percent (95 percent confidence interval, 81 to 93 percent), respectively. As important, the negative predictive values for any coronary artery disease and for left main artery or three-vessel disease were 81 percent (95 percent confidence interval, 73 to 89 percent) and 100 percent (95 percent confidence interval, 97 to 100 percent), respectively. Thus, in patients referred for their first x-ray coronary angiogram, 3D coronary CMR was highly accurate for the detection CAD of the proximal and middle segments. Many, including us, utilize such an approach when asked to rule out life-threatening left main or three-vessel disease [44].

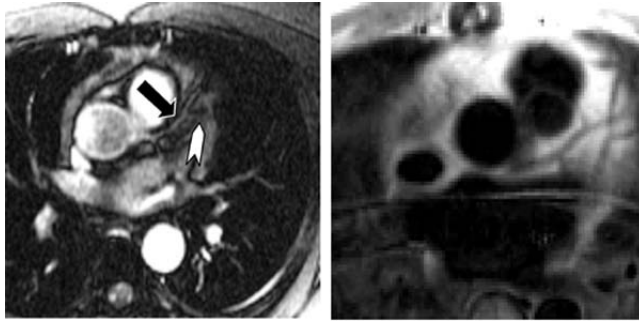


**Fig. (12).** A) The left main, proximal and mid sections of the LAD seen (arrow) using SSFP. A small portion of the diagonal vessel (chevron) is also appreciated in a patient with an angiographically normal LAD.

B) Spin-echo image of another patient showing similar anatomy.



**Fig. (13).** A 22 second image defining the thoracic aorta integrity of the right subclavian, left common carotid and left subclavian artery. Note is also made of three intact and widely patent saphenous vein graphs in this patient referred for post-CABG evaluation s/p Dor procure avoiding the need for invasive x-ray angiography.

## FUTURE CMR CONSIDERATIONS

### Diastolic Function by CMR

Paramount to the complete interrogation of LV myocardial function is the ability to evaluate the *entire* cardiac function: systolic and diastolic. Little systematic evaluation has been conducted in the evaluation of diastolic function using

CMR, since to date, the major emphasis has been on assessment of systolic function. Nonetheless, diastolic dysfunction is a state that accompanies up to 50% of ‘normal’ systolic function patients possibly 100% of those with ischemic cardiomyopathy, vexing their already precarious cardiovascular system. We performed a 3D CMR assessment of diastolic function utilizing a comparison with conventional echocardiography.

CMR’s spatial resolution, 3D nature and precision provide superiority over echocardiography (TTE) for systolic function and make it naturally provocative to compare. However, no assessment of diastolic function over a range of lusitropy has been performed by CMR. Limitations of diastolic function by TTE are manifest, yet it remains the *de facto* “gold standard”.

We hypothesized that by CMR lusitropic function was comparable to TTE but without the latter’s obligate acquisition limitations. While not confined to ischemic cardiomyopathy patients but we sought first to determine the intrinsic capability of CMR. We evaluated 31 subjects, age: 26-84 (male 21, female 10) including 10 controls *via* standard but optimized CMR (temporal resolution:  $19 \pm 3$ ms) using phase velocity mapping (PVM). All patients were successfully imaged by CMR to yield mitral diastolic filling patterns and velocities in an analogous technique to that employed by echocardiography. The representations of diastole were diverse: 11 impaired relaxation, 3 restrictive, 2 pseudonormalized, 3 EA fusions and 12 normal. Our sampling technique employed the following parameters: 3D mitral (MV) plane, 3D right upper pulmonary vein (PV). Two hour post CMR a blinded pulse wave Doppler TTE was performed (Philips 5500, Andover, MA). We showed that all mitral valves and pulmonary veins were imaged by CMR (31/31,100%) while TTE imaged all mitral valves (31/31,100%) but only 19/31 pulmonary veins (61%). No difference in acquisition plus offline processing time existed. Morphologically, CMR 100% correctly identified inflow abnormalities as assessed by TTE. Mitral valve E and A velocities by CMR were somewhat lower than TTE but well correlated ( $r=0.81$ ,  $p<0.05$ ). The E:A ratio and deceleration time (DT) were not statistically different between CMR and TTE and had excellent agreement by Bland-Altman analysis: Bias -0.29, and -10.3 for E/A and DT, (Fig. 14).

Morphologically, we saw homology between CMR and TTE despite very heterogeneous pathology with near exact inflow velocities. This was one of the first such demonstration and the most systematic characterization of patients with varied pathology by CMR yet, from this evaluation, albeit it early in the course, it can be seen that CMR, *via* phase velocity mapping can derive comparable diastolic indices to echocardiography [45, 46]. Given CMR’s 3D ability, it seems reasonable to predict far more sophisticated analyses are imminent. Given the advantages CMR provides for systole, it follows that diastolic applications appear equally possible paving the way for, not only more complex diastolic interrogations made possible by the functionality of CMR, but also applications specifically tailored for the ischemic cardiomyopathic patient.

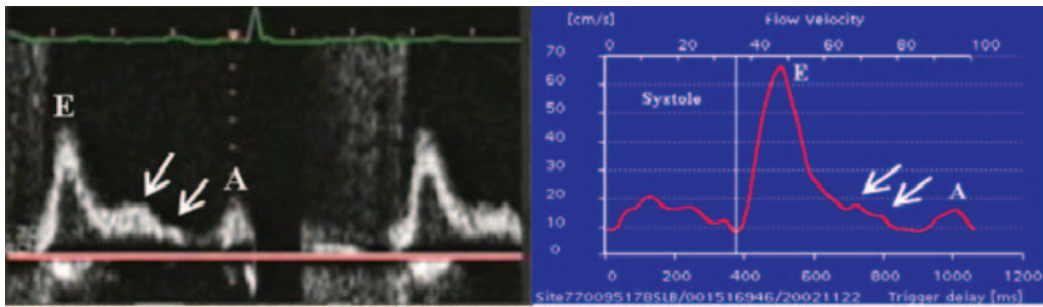


**Fig. (14).** Corresponding echocardiographic LV diastolic mitral filling patterns (A) with CMR derived phase velocity mapping acquired filling patterns (B) revealing, in both cases near exact replication of the restrictive pattern, confirming an adverse prognostic clinical finding. Note, the homology in the minutest of detail in the echocardiographic images molded by the CMR (arrows). Courtesy of Vikas Rathi, MD, Allegheny General Hospital, Pittsburgh, PA.

### Stem Cell Therapy; Uncharted Territory

In the future it is reasonable to believe that many patients will have a more predictable outcome following a myocardial infarction and LV remodeling can be thwarted, even forestalled. Unique advances into this precept are occurring on a monthly basis in the rapidly advancing science of stem cell replacement/regeneration therapy. Problematic in this noble pursuit is an imaging technique that is as refined as the science it seeks to describe. In this fashion, echocardiographic techniques have been relegated to the task but may serve as a paradoxical deterrent to the advancement of the field given their limited ability to describe accurately and *reproducibly* those intramyocardial actions that are beyond their detectable limits. CMR may offer help for the field given recent developments in magnetodendrimers [47], compounds that have both detectability by CMR and histology. For instance, in a classic paper mesenchymal stem cells were injected into an area of myocardium previously shown to have been infarcted by DHE. Over the course of several weeks progressive engraftment could be seen characterized both by CMR-visible iron particles and immunofluorescent-visible particles visible as a gradually spreading mid-myocardial zone with slow but definitive rearrangements to reorganize parallel to native myocardial fibers [48]. While this does not confirm contraction, it strongly supports such. It remains again for CMR to demonstrate that mesenchymal stem cells not only engraft but appear to intercalate within the perimesial fibers to effect mechanical contraction. Utilizing RF tissue tagging, mesenchymal cells were recently shown *via* myocardial circumferential strain (%S) to contract in a measurable and important manner as compared to a sham infarcted dog model [49]. The utility of CMR for this burgeoning field remains untapped.

### SVR Results Interpreted in Terms of an Energy Model

Recently, a mathematical model of the LV was developed by Shoucri, which describes the energy utilization of the LV [50, 51]. In this model, the LV is represented as a thick-walled cylinder capable of symmetric contraction. The work done in radially directed contraction and pressure generation is balanced against the product of myocardial elastance and the change in LV volume, Eq. 1 [45].

$$Dh - P = E(Ved - V) \quad \text{Eq. 1}$$

Where D is the radially resolved component of force produced by circumferential contraction of the LV, h is the

thickness of the myocardium, P is the instantaneous LV pressure, E is the instantaneous elastance of the myocardium, Ved is the end-diastolic LV volume and V is the instantaneous LV volume.

Evaluating the relationship at end-systole and relating the pressure-volume loop for an individual cycle to the ESPVR, the Shoucri model can be used to non-invasively describe the energy and elastance status of the LV, allowing optimal operating conditions to be determined, Figs. (15-17). The area encompassed by an individual pressure-volume loop (SW in Fig. 11) corresponds to the stroke work performed by the LV, which can be regarded as the "external work" performed. The area of triangle BE is proportional to the baseline metabolic energy requirement of the LV and can be regarded as the "internal" energy. LV elastance is represented by the slope of the ESPVR curve, and is termed Emax in Fig. (15). Similarly, the maximal aortic elastance occurs at end-systole and is represented diagrammatically by the slope, Eam, i.e. the "diagonal" of the pressure-volume loop. By considering the LV's energy requirements as it relates to

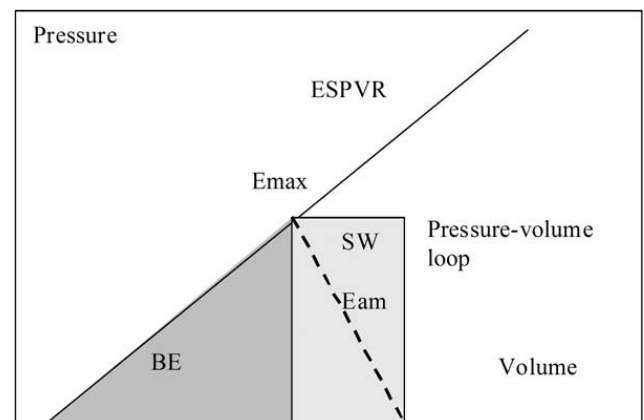


**Fig. (15).** The LV model developed from consideration of the mechanics of LV contraction. The cross-hatched rectangle represents an individual pressure-volume loop with ESPVR representing the end-systolic pressure volume relationship. Emax is the slope of the ESPVR curve, representing maximal myocardial elastance. Similarly Eam is the slope of the dashed line representing arterial elastance at end systole. The area enclosed by the pressure-volume loop represents the stroke work (SW) performed by the LV. The shaded triangular area, BE, represents the baseline metabolic energy utilization of the LV.

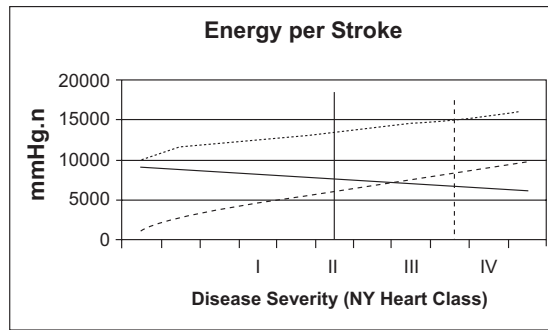


**Fig. (16).** Simulated data showing the contribution of stroke work (solid line), baseline energy (dot-dash line), and total energy (dotted line) with heart class status. Indicated by the vertical lines are the mean patient status pre SVR (dashed) and post SVR (solid), indicating a progression towards normal. In this case, the EF increased from 29% to 39% and the total energy decreased by 9%.

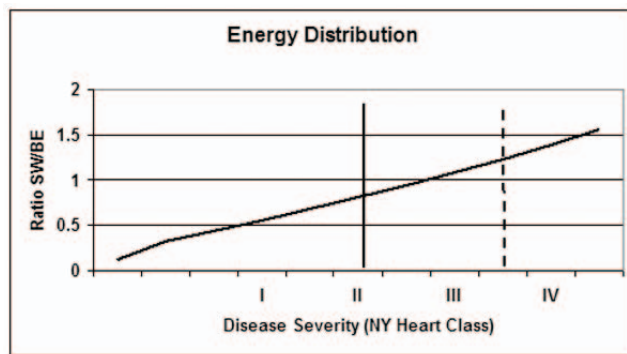


**Fig. (17).** Simulated data showing the ratio of stroke work to baseline energy with heart class status. Indicated by the vertical lines are the mean patient status pre SVR (dashed) and post SVR (solid), indicating a progression towards normal. Interestingly, the SVR procedure had restored conditions such that SW was a greater contribution than BE.

the stroke volume generated, the ejection efficiency can be calculated. According to the Shoucri model, ejection efficiency is maximized when the ratio  $E_{max}:E_{am}$  is 2:1. Similarly, stroke work is maximal when  $E_{max}:E_{am}$  is 1:1, which sacrifices efficiency for size of the volume ejected. The ratio of  $E_{max}:E_{am}$  is termed the “Ventricular-Aorto Coupling Efficiency”. This ratio is a measure of energy wastage, since an inefficient ventricular-aorto coupling factor necessarily dissipates energy in the form of heart.

To simulate the progression towards HF, we modeled likely changes in ventricular parameters including ESV, EDV, ESBP and EDBP. In our model, the ESV increased from 100 ml to 200 ml, the EDV increased from 40 ml to 156 ml, the EF decreased from 60% to 22%, and the stroke volume decreased from 60 ml to 44 ml. Using these values we calculated energy model parameters including EF, baseline energy (BE), stroke work (SW) and total energy. Based on RESTORE Group analysis of SVR patients the EF increases from 29.6 +/- 11.0% preoperatively to 39.5 +/- 12.3% postoperatively [52]. In terms of our simulated energy model parameters, this corresponds to a mean decrease in BE of 26% and a mean increase in SW of 12%, with the net work decreasing by only 9%, Fig. (16). Compared to nor-

mal, these values are still elevated. In the normal case, BE is approximately one third of SW, and by matching the EF values reported in the pre SVR group, the mean ratio of BE/SW was 1.23 representing a reversal of energy distribution compared to normals. Post SVR the BE/SW ratio decreased to 0.8, representing a progression towards normalization, but clearly still in the abnormal range, Fig. (17).

## CONCLUSION

The impact of CMR has been well documented since its inception nearly 20 years ago and has gained credence with each passing year. To appreciate the impact that future key developments will have CMR imaging, it is instructive to consider its present status. CMR has passed the threshold of being used primarily by innovators, and is now deep into the adopter stage. Though to reach this threshold, it has taken many years, its adoption by early majority users is expected to accelerate the growth of CMR, now nowhere more evident than in the field of cardiovascular surgery, especially as related to advanced therapeutics such as the SVR procedure. A number of important factors govern its natural growth potential, including physician education and credentialing, scanner availability, technology, and reimbursement policies. However, the intrinsic dimensional accuracy of CMR, coupled with its high level of reproducibility, make it ideal for inclusion in surgical trials, potentially with dramatic reductions in trial duration and the number of subjects required. This will have unexpected consequence of earlier submission of data for FDA approval and adoption into the mainstream.

Clinically, there are a number of clinical and research applications for which CMR is widely regarded as being the diagnostic test of choice or ‘gold standard’. Software and hardware developments that speed up the basic CMR procedure are being incorporated into scanners, extending the functionality of routine applications such as flow imaging and tissue-tag visualization. Exciting areas that are close to routine application include coronary artery imaging, and evaluation of myocardial perfusion and viability status [53, 54]. Taken together, CMR offers those critical and highly desirous attributes that the National Heart, Lung, and Blood Institute workshop entitled “Form and Function: New Views on Development, Diseases, and Therapies for the Heart” convened on April 25- 26, 2002, in Bethesda, Maryland called for [55]. The objective by the NHLBI was to jump-start a venture to understand the importance of structure and functional relationships of the intact ventricles from both the basic science and clinical perspectives and to define where progress is most urgently needed while planning research programs that will most effectively integrate understanding of functional geometry into therapy of human heart disease. It is worthwhile noting that those attributes are well found within the confines of CMR.

Finally, the clinical incorporation of CMR metrics into the mainstream of key cardiac parameters deemed to have a singular importance when judged in the terms of morbidity and mortality, continue to offer insight and direction for those who use them. The rapidly evolving field of surgical correction of the ischemic cardiomyopathic patient is witness to this. As surgical reconstruction therapy evolves, with the SVR as its’ paradigm, the utility of this progression can, not

only be discerned but influenced. When added to CMR's ability to define cardiac parameters not thought of, indeed undetectable by current traditional modalities, the utility of such an approach is translucent. Underscoring this, the financial consequences for answering the clinical question correctly the *first* time despite a slightly higher upfront price have long-term markedly favorable socioeconomic ramifications. We refer to those as tangible vs. intangible benefits. The earlier identification of disease with the insightful direction (or redirection) of germane therapeutic directions unambiguously outlined offers a solution for what the medical imaging world may be looking for. In an ischemic cardiomyopathy patient with limited options, the rich linkage between advanced imaging and SVR is reassuring that scientific advances can have synergistic effects towards a common goal and good for the patient.

#### ACKNOWLEDGEMENTS

Special thanks is given to the many fine investigators with whom we have had the pleasure of working with including Gerald Buckberg MD, Agustino Meduri MD, Vikas K. Rathi MD, Alistair A. Young PhD, Eduardo Kortright PhD, Connie Athanasuleas MD, Al Stanley MD, Lou J. Dell'Italia MD, and Gerald M. Pohost MD, with whom this work would not have been possible.

#### REFERENCES

- [1] Pohost GM, Biederman RW. The role of cardiac MRI stress testing: "Make a better mouse trap...". *Circ* 1999; 100: 1676-9.
- [2] Biederman, RWW, Pohost GM. Pathology of the dilated cardiomyopathy, Chapter 47. In: Pohost GM, Shaw P, O'Rourke R, Berman D, Eds. *Imaging in Cardiovascular Medicine*, Lippincott: Williams and Wilkins 1999.
- [3] Biederman RWW, Pohost GM. Imaging of dilated cardiomyopathy. Chapter 48. In: Pohost GM, Shaw P, O'Rourke R, Berman D, Eds. *Imaging in Cardiovascular Medicine*. Lippincott: Williams and Wilkins 1999.
- [4] Sandiford FM, Cooley DA. Resection of left ventricular aneurysm. Report of 277 patients. *G Ital Cardiol* 1975; 5: 173-83.
- [5] Jatene AD. Left ventricular aneurysmectomy: resection or reconstruction. *J Thorac Cardiovasc Surg* 1985; 89: 321-31.
- [6] Dor V, Montiglio F, Sabatier M, *et al.* Left ventricular shape changes induced by aneurysmectomy with endoventricular circular patch plasty reconstruction. *Eur Heart J* 1994; 15: 1063-9.
- [7] Cranney GB, Lotan CS, Dean L, Baxley W, Bouchard A, Pohost GM. Left ventricular volume measurement using cardiac axis NMR imaging: validation by calibrated ventricular angiography. *Circulation* 1990; 82: 154-63.
- [8] Bottini PB, Carr AA, Prisant LM, Flickinger FW, Allison JD, Gottdiener JS. Magnetic resonance imaging compared to echocardiography to assess left ventricular mass in the hypertensive patient. *Am J Hypertens* 1995; 8: 221-8.
- [9] Biederman R, Aldrich M, Rogers W, *et al.* Does the Adage, "there is safety in numbers" Lead us astray? an MRI remodeling study. *J Cardiovasc Magn Reson* 2002; 4: 177.
- [10] Poon M, Fuster V, Fayad Z. Cardiac magnetic resonance imaging: a "one-stop-shop" evaluation of myocardial dysfunction. *Curr Opin Cardiol* 2002; 17: 663-70.
- [11] Biederman RWW, Doyle M, Young AA, *et al.* Evidence for disproportionate myocardial dysfunction in the septum in hypertensive left ventricular hypertrophy. *J Am Coll Cardiol* 1998; 97: 345A.
- [12] Biederman RWW, Doyle M, Young A, *et al.* Regional heterogeneity in 3D myocardial shortening in hypertensive LV hypertrophy: MR tagging substudy to life. *Hypertension* 2008; 52: 279-86.
- [13] Biederman RWW, Doyle M, Yamrozik J, *et al.* Physiologic compensation is supranormal in compensated aortic stenosis: does it return to normal after aortic valve replacement or is it blunted by coexistent Coronary Artery Disease? *Circulation* 2005; 112(suppl 1): I-429-I-436.
- [14] Nakano K, Swindle MM, Spinale FG, *et al.* Depressed contractile dysfunction due to canine mitral regurgitation improves after correction of the volume overload. *J Clin Invest* 1991; 87: 2077-86.
- [15] Shaw P, Biederman. RWW. Hypertrophic cardiomyopathy. Chapter 45. In: Pohost GM, Shaw, P, O'Rourke, R, Berman, D, Eds. *Imaging in Cardiovascular Medicine*, Lippincott: Williams and Wilkins 1999.
- [16] Devereux RB, Roman MJ, de Simone G, *et al.* Relations of left ventricular mass to demographic and hemodynamic variables in American Indians: the Strong Heart Study. *Circulation* 1997; 96: 1416-23.
- [17] Bellenger NG, Burgess MI, Ray SG, *et al.* Comparison of left ventricular ejection fraction and volumes in heart failure by echocardiography, radionuclide ventriculography and cardiovascular magnetic resonance; are they interchangeable? *Eur Heart J* 2000; 21: 1387-96.
- [18] Darasz KH, Underwood SR, Bayliss J, *et al.* Measurement of left ventricular volume after anterior myocardial infarction: comparison of magnetic resonance imaging, echocardiography, and radionuclide ventriculography. *Int J Cardiovasc Imaging* 2002; 18: 135-42.
- [19] Malm S, Frigstad S, Sagberg E, Larsson H, Skjaerpe T. Accurate and reproducible measurement of left ventricular volume and ejection fraction by contrast echocardiography: a comparison with magnetic resonance imaging. *J Am Coll Cardiol* 2004; 1; 44: 1030-5.
- [20] Hunold P, Vogt FM, Heemann UW, Zimmermann U, Barkhausen J. Myocardial mass and volume measurement of hypertrophic left ventricles by MRI--study in dialysis patients examined before and after dialysis. *J Cardiovasc Magn Reson* 2003; 5: 553-61.
- [21] Gaudio C, Tanzilli G, Mazzarotto P, *et al.* Comparison of left ventricular ejection fraction by magnetic resonance imaging and radionuclide ventriculography in idiopathic dilated cardiomyopathy. *Am J Cardiol* 1991; 67: 411-5.
- [22] Pitt B, Reichek N, Willenbrock R, *et al.* Effects of eplerenone, enalapril, and eplerenone/enalapril in patients with essential hypertension and left ventricular hypertrophy: the 4E-left ventricular hypertrophy study. *Circulation* 2003; 108(15): 1831-8.
- [23] Mollet NR, Dymarkowski S, Volders W, *et al.* Visualization of ventricular thrombi with contrast-enhanced magnetic resonance imaging in patients with ischemic heart disease. *Circulation* 2002; 106(3): 2873-6.
- [24] Doyle M, Kortright E, Anayiotos AS, *et al.* Rapid velocity-encoded cine imaging with turbo-BRISK. *J Cardiovasc Magn Reson* 1999; 1: 223-32.
- [25] Doyle M, Rayarao G, Yamrozik J, *et al.* Validation of rapid high resolution MRI assessment of left ventricular function. In: *Proceedings of Seventh Annual SCMR Scientific Sessions/Euro CMR 2004 Meeting*, February 13-15, 2004, Barcelona, Spain.
- [26] Biederman RWW, Doyle M, Fuisz AR, *et al.* CMR analysis of the dor left ventricular surgical reconstruction for non-ischemic dilated cardiomyopathy. *J Cardiovasc Magn Reson* 1999; 3: 268.
- [27] Rademakers FE, Rogers WJ, Guier WH, *et al.* Relation of regional cross-fiber shortening to wall thickening in the intact heart. three-dimensional strain analysis by NMR tagging. *Circulation* 1994; 89: 1174 - 82.
- [28] Biederman RW, Doyle M, Young AA, *et al.* Marked regional left ventricular heterogeneity in hypertensive left ventricular hypertrophy patients: a losartan intervention for endpoint reduction in hypertension (LIFE) cardiovascular magnetic resonance and echocardiographic substudy. *Hypertension* 2008; 52: 279-86.
- [29] Pan L, Lima JA, Osman NF. Fast tracking of cardiac motion using 3D-HARP. *Inf Process Med Imaging* 2003; 18: 611-22.
- [30] Corron NJ, Schronrock HE, Amos JR, *et al.* Automated magnetic resonance imaging tag tracking algorithm for regional wall motion analysis. *J Cardiovasc Magn Reson* 1999; 3: 284.
- [31] Biederman R, Doyle M, Kortright E, Fuisz A, Honey D, Pohost G. 1D misguides 3-D: an echocardiographic and magnetic resonance imaging comparison. *J Am Coll Cardiol* 2002; 39: 150A.
- [32] Biederman RWW, Doyle M, Kortright E, Fuisz AR, Honey DJ, Pohost GM. Does the 1D end-diastolic dimension misguide the estimation of 3D end-diastolic volume in patients with ischemic cardiomyopathy? *Magn Reson Mater Phys Biol Med* 2000; 11(Suppl 1): 36.

- [33] Biederman R, Doyle M, Young A, *et al.* Regional mechanics and reverse remodeling after LV reconstruction surgery: A one year 3-D MRI analysis. *Suppl II Circ* 2001; 104: 336.
- [34] Biederman R, Doyle M, Young A, *et al.* Global and regional mechanics together with reverse remodeling after LV reconstruction surgery: a one year 3-D MRI analysis. *J Cardiovasc Magn Reson* 2002; 4: 142-3.
- [35] Kloner RA, Bolli R, Marban, *et al.* Medical and cellular implications of stunning, hibernation, and preconditioning. An NHLBI Workshop. *Circulation* 1998; 97: 1848-67.
- [36] Wagner A, Mahrholdt H, Holly TA, *et al.* Contrast-enhanced CMR and routine single photon emission computed tomography (SPECT) perfusion imaging for detection of subendocardial myocardial infarcts: an imaging study. *Lancet* 2003; 361: 374-9.
- [37] Klein C, Nekolla SG, Bengel FM, *et al.* Assessment of myocardial viability with contrast-enhanced magnetic resonance imaging. Comparison with positron emission tomography. *Circulation* 2002; 105: 162-7.
- [38] Kim RJ, Wu E, Rafael A, *et al.* The use of contrast-enhanced magnetic resonance imaging to identify reversible myocardial dysfunction. *N Engl J Med* 2000; 343: 1445-53.
- [39] Rogers W, Rhodes D, Biederman R, *et al.* "Timing is everything": time course of myocardial delayed enhancement after acute MI. *Suppl II Circ* 2001; 104: 639.
- [40] Doyle M, Ripple J, Yamrozik J, *et al.* Regions of delayed hyperenhancement demonstrate long term improved function. Scientific Sessions of the American Heart Association: Chicago, IL: 2002 (abst).
- [41] Selvanayagam JB, Kardos A, Francis JM, *et al.* Value of delayed-enhancement cardiovascular magnetic resonance imaging in predicting myocardial viability after surgical revascularization. *Circulation* 2004; 110: 1535-41.
- [42] Uretsky B. ATLAS trial: acute coronary findings at autopsy in HF patients with sudden death. *Circulation* 2000; 102: 611-6.
- [43] Biederman RWW, Fuisz AR, Pohost GM. Magnetic resonance image. *Curr Opin Cardiol* 1998; 13: 430-7.
- [44] Kim WY, Danias PG, Stuber M, *et al.* Coronary magnetic resonance angiography for the detection of coronary stenoses. *N Engl J Med* 2001; 27: 1863-9.
- [45] Rathi VK, Doyle M, Yamrozik J, *et al.* Cardiovascular 3D MRI assessment of diastolic dysfunction: a comparison with echocardiography. *Circulation* 2004; 110(17, Suppl III): 2962.
- [46] Rathi VK, Doyle M, Yamrozik J, *et al.* Routine evaluation of left ventricular diastolic function by cardiovascular magnetic resonance: a practical approach. *J Cardiovasc Magn Reson* 2008; 10: 36.
- [47] Kraitchman DL, Heldman AW, Atalar E, *et al.* *In vivo* magnetic resonance imaging of mesenchymal stem cells in myocardial infarction. *Circulation* 2003; 107: 2290-93.
- [48] Hill JM, Dick AJ, Raman VK, *et al.* Serial cardiac magnetic resonance imaging of injected mesenchymal stem cells. *Circulation* 2003; 108: 1009-14.
- [49] Gallegos RP. Improved regional function after stem cell treatment in the canine chronic infarct model. *J Cardiovasc Magn Reson* 2004; 6: 56.
- [50] Shoucri RM. Pressure-volume relation in left ventricle. *Am J Physiol* 1991; 260: H282-H91.
- [51] Shoucri RM. Performance of the left ventricle based on pressure-volume relation. *J Biomed Eng* 1990; 12: 482-8.
- [52] Athanasuleas CL, Buckberg GD, Stanley AW, *et al.* Surgical ventricular restoration in the treatment of congestive heart failure due to post-infarction ventricular dilation. *J Am Coll Cardiol* 2004; 44: 1439-45.
- [53] Pohost GM, Biederman RW, Doyle M. Cardiovascular magnetic resonance imaging and spectroscopy in the new millennium. *Curr Probl Cardiol* 2000; 25: 525-620.
- [54] Doyle M, Biederman RW. Future prospects in magnetic resonance imaging. *Curr Cardiol Rep* 2004; 6: 70-5.
- [55] Buckberg GD, Weisfeldt ML, Ballester MB, *et al.* Left ventricular form and function. scientific priorities and strategic planning for development of new views of disease. *Circulation* 2004; 110: e333-e6.

Received: April 28, 2008

Revised: January 05, 2009

Accepted: February 03, 2009

© Biederman and Doyle; licensee *Bentham Open*.

This is an open access article licensed under the terms of the Creative Commons Attribution Non-Commercial License (<http://creativecommons.org/licenses/by-nc/3.0/>) which permits unrestricted, non-commercial use, distribution and reproduction in any medium, provided the work is properly cited.